IOP Conf. Series: Materials Science and Engineering **278** (2017) 012060 doi:10.1088/1757-899X/278/1/012060

Lumped Multi-Bubble Analysis of Injection Cooling System for Storage of Cryogenic Liquids

Pritam Saha and Pavitra Sandilya

Cryogenic Engineering Centre, Indian Institute of Technology Kharagpur, Kharagpur 721302, West Bengal, India

E-mail: profsandilya@gmail.com

Abstract. Storage of cryogenic liquids is a critical issue in many cryogenic applications. Subcooling of the liquid by bubbling a gas has been suggested to extend the storage period by reducing the boil-off loss. Liquid evaporation into the gas may cause liquid subcooling by extracting the latent heat of vaporization from the liquid. The present study aims at studying the factors affecting the liquid subcooling during gas injection. A lumped parameter model is presented to capture the effects of bubble dynamics (coalescence, breakup, deformation etc.) on the heat and mass transport between the gas and the liquid. The liquid subcooling has been estimated as a function of the key operating variables such as gas flow rate and gas injection temperature. Numerical results have been found to predict the change in the liquid temperature drop reasonably well when compared with the previously reported experimental results. This modelling approach can therefore be used in gauging the significance of various process variables on the liquid subcooling by injection cooling, as well as in designing and rating an injection cooling system.

1. Introduction

Cryogenic liquids boil off easily due to their low boiling points. Hence prevention of revaporization during their storage over long period like in space exploration, sea transport etc., poses a major technological challenge. Zero Boil-Off (ZBO) tanks have been developed for such purpose. However, in situations where high payload and vibrations due to engine operation are unacceptable, a simpler way via liquid subcooling has been proposed. The subcooling of liquid can be done by using cryogenic liquid densification [1–3], thermodynamic cryogen subcooler (TCS) [4, 5] and by injecting an almost insoluble, immiscible and non-condensable gas [6–11]. Among these, the liquid subcooling by gas injection, called injection cooling, is the simplest and involves less moving machineries. This method of boiling suppression is simple but efficient, especially when space is at premium and amount of subcooling needed is low. Gas injection also inhibits any thermal stratification in the storage vessel due to ambient heat inleak. Suppression of boiling on injection of a gas was first reported by Minkoff et al. [6]; they observed elimination of boiling in liquid nitrogen (LN2), liquid oxygen (LOX), liquid air, liquid argon (LAr) by injecting helium, hydrogen, argon, oxygen, air and neon gas through the liquids.

In the present paper a simplified lumped multi-bubble approach has been adopted to evaluate the cooling performance of injection cooling and to identify the effects of gas flow rate and gas injection temperature on cooling performance. There exist many flow regimes in two phase gas-liquid flow. Among them bubbly flow provides larger specific gas-liquid interfacial area to the

heat and mass transport than other flow regimes. A numerical model has been developed based on mass and energy balance between the gas and the liquid considering gas holdup in bubble column. This model captures all the essential transport phenomena involved during injection cooling. This study would help in identifying the range and sensitivity of the aforesaid operating variables on injection cooling.

2. Working principle

Injection cooling operation is shown schematically in Fig. 1. Here the liquid is kept in a storage vessel and the gas is passed through the liquid by a suitable gas sparger or bubbler. The gas moves upward through the liquid before exiting out of the vessel. Insulations are provided to eliminate/minimize the heat inleak from the ambient.

Figure 2 depicts the overall heat interactions between the liquid and the gas phase that could bring about liquid cooling. When an insoluble or sparingly soluble gas is bubbled through a liquid, difference between the saturation pressure of the liquid at the liquid temperature and partial pressure of the liquid component inside the gas bubble makes the liquid evaporate into the gas bubble. In absence of any external heating source, the liquid derives the necessary heat for its vaporization from liquid bulk thereby reducing its internal energy and thus effecting its cooling. On the other hand, the gas bubbles tend to warm up due to the latent heat transfer from the liquid. This interphase heat and mass transfer are mainly affected by the two phase bubble hydrodynamics. The overall performance of the injection cooling system thus depends on several operating variables like gas flow rate and temperature, sparger hole size and sparger position etc.

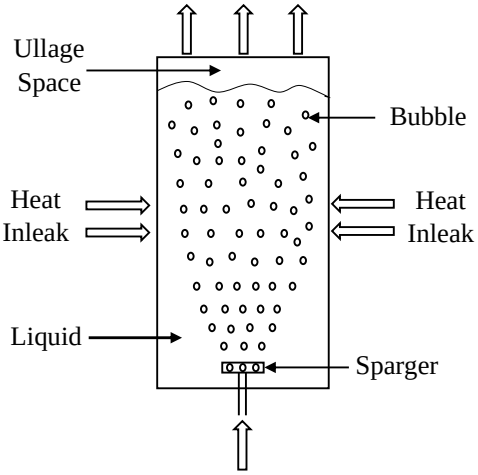

Figure 1. Schematic of bubbling system for liquid subcooling.

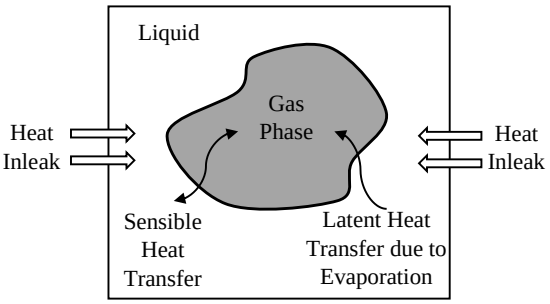

Figure 2. Mechanism of heat and mass exchange between liquid and gas.

3. Earlier studies

Only few studies on injection cooling have been reported. Performance of injection cooling has studied both theoretically and experimentally. Larsen et al. [7] developed an analytical solution and conducted experiments on injection cooling using LOX-GHe, LN2-GHe, and LOX-N2 systems. They showed the dependency of subcooling on gas flow rate. Schmidt [8] through their experiments on LH2-GHe system, showed the effect of gas injection temperature and gas flow rate on liquid cooling. Analytical modeling based on instantaneous heat and mass transfer was validated by Cho et al. [10] with the experimental results obtained for LOX-GHe system at different gas flow rates. Jung et al. [11] modeled the injection cooling system based on instantaneous heat transfer and transient mass transfer and validated the model with the experimental results obtained from LOX-GHe system for different gas flow rate. Analytical and

experimental results on the cooling performance of LN2, LOX and LH2 by bubbling helium gas considering finite heat transfer and instantaneous mass transfer were reported by Ramesh and Thyagarajan [12]. Sandilya et al. [13] presented a CFD based study on the bubble movement during injection cooling to demonstrate the significance of bubble dynamics on liquid cooling.

4. Modeling

The injection cooling process is equivalent to the transport phenomena occurring in a bubble column that is commonly used in chemical and allied industries. Heat and mass transfer in such columns are governed by the bubble dynamics and other two phase hydrodynamics. In the lumped parameter approach for modeling the injection cooling system, the associated heat and mass transfer may be modeled considering the gas hold up and mean diameter of the bubbles. In the present work, the modeling has been performed to determine the time variation of liquid temperature by writing energy balance for liquid and gas phase.

4.1. Energy balance for liquid and gas phase

In injection cooling the temperature of the liquid is expected to drop primarily due to the latent heat transfer from the liquid to gas bubbles during liquid evaporation. This will tend to heat up the bubble thereby causing a sensible heat transfer from the bubble to the liquid. Cooling will occur if the rate of evaporative mass transfer is higher than the sensible heat transfer. Moreover, the rate of liquid cooling will also be affected by the heat inleak to the liquid from the ambient. Energy balance equations for the gas bubbles and the liquid are given in Eqs. 1 and 2.

Liquid side

$$\frac{d}{dt}\left(m_l C_{p,l} \Delta T_l\right) = \left(\dot{q}_{g-l} + \dot{q}_{amb} - \dot{q}_{evp}\right) \tag{1}$$

Gas side

$$\frac{d}{dt}\left(m_g C_{p,g} \Delta T_g\right) = \left(\dot{q}_{evp} - \dot{q}_{g-l}\right) \tag{2}$$

The initial and boundary conditions are as follows.

$$\text{At} \quad t = 0, T_l = T_{l,0}, T_g = T_{g,0}$$

$$\text{At} \quad t = 0, m_l = m_{l,0}, m_g = m_{g,0}$$

4.2. Bubble dynamics

Bubble behavior is dictated by their size, rise velocity, interactions, breakage, coalescence and flow trajectory. These factors have been approximated as given below.

4.2.1. Gas holdup and bubble diameter When a gas is injected into the liquid through an orifice at a comparatively lower flow rate, bubble formation takes place at the orifice mouth followed by the growth, detachment and rise through the liquid. The specific gas-liquid interfacial area or the specific surface area offered by all the bubbles for heat and mass transfer between liquid and bubbles can be predicted by Eq. 3.

$$a_s = \frac{6\varepsilon_g}{d_{vs}} \tag{3}$$

Gas holdup is one of the most important parameters that characterize the two phase bubble hydrodynamics. It is the amount of gas fraction present in the gas-liquid mixture. It has been estimated from the correlation suggested by Viswanathan and Rao [14] as given in Eq. 4.

$$\varepsilon_g = 0.5 {v_g}^{0.8} {v_t}^{-0.4} (0.5 g d_c)^{-0.2} \tag{4}$$

The Sauter mean diameter of the bubbles can be determined from Eq. 5 proposed by Akita and Yoshida [15].

$$d_{vs} = 26 d_c \mathrm{Bo}^{-0.50} \mathrm{Ga}^{-0.12} \mathrm{Fr}^{-0.12} \tag{5}$$

4.2.2. Bubble terminal velocity and residence time Bubble breakup, deformation and coalescence effects have been considered for evaluating the specific gas -liquid interfacial area. When bubbles rise through the liquid, they are acted upon by several external forces like drag force, lift force, virtual mass force and wall force, which determine their rise velocity and their flow trajectory. On balancing of these forces, the bubbles attain a constant terminal velocity. Clift et al. [16] suggested following correlations to find the terminal velocity of single bubble originating from an upward facing orifice placed at the bottom of the liquid column.

$$v_t = \frac{\mu_l}{\rho_l d_{vs}} \mathrm{Mo}^{-0.149} \left(0.94 {H_0}^{0.747} - 0.857\right) \text{when } (2 < H_0 \leq 59.3) \tag{6}$$

$$v_t = \frac{\mu_l}{\rho_l d_{vs}} \mathrm{Mo}^{-0.149} \left(3.42 {H_0}^{0.441} - 0.857\right) \text{when } (H_0 > 59.3) \tag{7}$$

4.3. Interphase heat transfer
In injection cooling, the gas may be injected at a temperature same as, or higher than the liquid temperature. In both the cases the sensible heat transfer will take place from the gas to the liquid due the establishment of a thermal gradient between the liquid and the gas. The sensible heat transfer from the gas to the liquid can be estimated from the Eq. 8.

$$\dot{q}_{g-l} = h_l a_s \varepsilon_g V_t \left(T_g - T_l\right) \tag{8}$$

The heat transfer coefficient in two phase flow varies with the type of gas-liquid system. The liquid side heat transfer coefficient (h_l) in Eq. 8 can be obtained from the Eq. 9 as reported by Deckwer [17].

$$\mathrm{St} = 0.1 \left(\mathrm{Re}_c \mathrm{Fr} \mathrm{Pr}^2\right)^{-0.25} \tag{9}$$

4.4. Ambient heat leak
The heat inleak from the ambient to the liquid can be estimated from Eq. 10.

$$\dot{q}_{amb} = 2\pi K_{ins} L_c \frac{T_{amb} - T_l}{\ln\left(\frac{r_{ins,o}}{r_{ins,i}}\right)} \tag{10}$$

Here the radiative heat transfer has been neglected by considering the inclusion of a reflecting surface in the insulation.

4.5. Interphase mass transfer
The rate of latent heat transfer from the liquid can be determined from Eq. 11.

$$\dot{q}_{evp} = \dot{m}_{evp} h_{fg} \tag{11}$$

The rate of liquid evaporation into the gas is caused by the difference between the vapour pressure of the liquid and partial pressure of the liquid vapour inside the gas bubble. This rate can be determined from Eq. 12.

$$\dot{m}_{evp} = k_g a_s \varepsilon_g V_t \left({P_A}^{Sat} - p_{\mathrm{A},g}\right) \tag{12}$$

The mass transfer coefficient in Eq. 12 has been estimated using the correlation suggested by Saboni et al. [18].

$$\mathrm{Sh} = 6.57 + \left(\frac{\mathrm{Re}_d \mathrm{Sc}}{8.35 + 0.0125(\mathrm{Re}_d \mathrm{Sc})^{1.66}} \right)^2 \tag{13}$$

5. Numerical solution strategy

Equations 1 and 2 have been solved using an in-house code written in Fortran 95. The coupled set of energy balance equations have been solved employing Euler explicit method. The temperatures at any time instant have been determined from Eq. 14 and 15.

$$T_l^{(n+1)} = T_l^n + \left(\dot{q}_{g-l} + \dot{q}_{amb} - \dot{q}_{evp} \right)^n \frac{\Delta t}{(m_l C_{p,l})^n} \tag{14}$$

$$T_g^{(n+1)} = T_g^n + \left(\dot{q}_{evp} - \dot{q}_{g-l} \right)^n \frac{\Delta t}{(m_g C_{g,l})^n} \tag{15}$$

The time-step independence study have been carried out for each set of operating conditions to check the invariability of the reported results with respect to the time step (Δt).

6. Results and discussion

The model has been validated with the experimental results reported by Ramesh and Thyagarajan [12]. The operating parameters and system configurations used for simulation are listed in Table 1 and Table 2.

Table 1. System configurations used for simulation and validation [12].

System configuration	Values
Height of working liquid (m)	0.9
Column diameter (m)	0.9
Orifice diameter (m)	0.002
Number of orifices	40

Table 2. Operating variables used for simulation and validation [12].

Operating variables	Values
Pressure (atm)	1.0
Mass flow rate of gas (g/s)	15, 20 and 25
Gas temperature (K)	85, 91, 150 and 295
Liquid temperature (K)	91 (LOX) and 78 (LN2)
Mass of liquid (kg)	650
Heat inleak (W)	220

The time step used for the simulation is 0.1 second. The important process parameters like terminal velocity, heat transfer coefficient and mass transfer coefficient have been calculated from Eqs. 6-7, Eq. 9 and Eq. 13 respectively with respect to different operating conditions and given in Table 3.

Table 3. Calculated values of terminal velocity, heat and mass transfer coefficient with respect to different operating conditions.

Sl. No.	Liquid	Gas flow rate (g/s)	Gas injection temp. (K)	Terminal velocity (m/s)	Heat transfer coefficient (W/m^2K)	Mass transfer coefficient (m/s)
1	LOX	15	91	0.145-0.148	2882.47-2901.70	$2.19x10^{-02}$-$1.72x10^{-02}$
2	LOX	20	91	0.142-0.146	3097.41-3116.74	$2.20x10^{-02}$-$1.57x10^{-02}$
3	LOX	25	91	0.140-0.144	3275.12-3289.63	$2.21x10^{-02}$-$1.45x10^{-02}$
4	LOX	25	150	0.140-0.144	3275.12-3294.85	$2.21x10^{-02}$-$1.55x10^{-02}$
5	LOX	25	295	0.140-0.144	3275.12-3296.16	$2.21x10^{-02}$-$1.80x10^{-02}$
6	LN2	25	91	0.460-0.465	3593.42-3582.24	$8.57x10^{-04}$-$8.02x10^{-04}$
7	LN2	25	150	0.460-0.465	3593.42-3582.44	$8.57x10^{-04}$-$8.03x10^{-04}$
8	LN2	25	295	0.460-0.465	3593.42-3582.97	$8.57x10^{-04}$-$8.05x10^{-04}$

Figure 3 depicts the variation of LOX temperature with respect to time at gas flow rates of 15, 20 and 25 g/s and a gas injection temperature of 91 K. It validates the results obtained from the simulation with the experimental results reported by Ramesh and Thyagarajan [12].

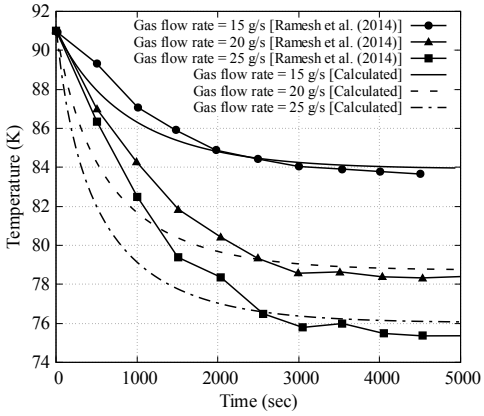

Figure 3. Variation of LOX temperature at gas flow rates of 15, 20 and 25 g/s and gas injection temperature of 91 K.

The rate and extent of cooling increase with increase in the gas flow rate. Higher gas flow rate gives rise to more bubbles that increases effective area for heat and mass transfer, while reduce contact time between gas and liquid. The temperature variation in Fig. 3 indicates that the latent heat transfer predominates the combined effect of the sensible heat transfer and ambient heat inleak.

Figures 4 and 5 show the variation in liquid temperature with respect to time at a gas flow rate of 25 g/s and a gas injection temperature of 85 K, 150 K and 295 K for LOX and LN2 respectively.

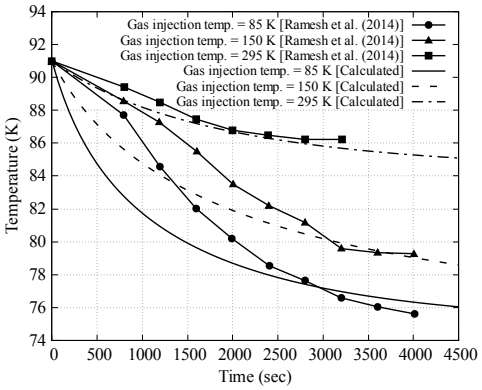

Figure 4. Variation of LOX temperature at a gas flow rate of 25 g/s and gas injection temperatures of 91, 150 and 295 K.

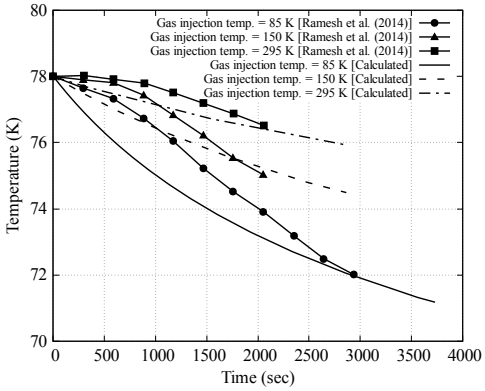

Figure 5. Variation of LN2 temperature at a gas flow rate of 25 g/s and gas injection temperatures of 91, 150 and 295 K.

From these figures, it is observed that cooling of liquid takes place even when the temperature of the injected gas is higher than the liquid saturation temperature at the corresponding pressure. However, higher gas injection temperature lowers the rate and extent of liquid cooling by increasing the sensible heat transfer from the gas to liquid which tends to heat up the liquid. Because evaporation continues at higher gas injection temperature also, transfer of latent heat from liquid to gas tends to cools down the liquid. At higher gas injection temperature, part of the latent heat counters the effect of the sensible heat transfer from the gas and the rest provides cooling to the liquid. Due to this at higher gas injection temperatures, extent of cooling decreases. Cooling is more for LOX than LN2 under similar operating conditions because the latent heat of vaporization for LN2 is less than that of LOX.

In all the cases, rate of cooling is higher at the beginning of injection cooling process, then reduces and finally reaches zero. This is because, in the beginning the saturation pressure of the liquid is maximum at the corresponding liquid temperature. As the liquid cools, the saturation pressure of the liquid starts to fall. Also partial presence of the liquid component increases in the bubbles. These decrease the driving force for evaporation and hence reduces the liquid cooling rate. The detailed fluid dynamic and transport behavior have been taken into account by multiplying a correction factor with the heat and mass transfer coefficient.

The model seems to underpredict the observed values. The reasons are two-fold. Firstly, the temperature and flow rate for model validation were not mentioned by the authors, and hence were deduced based on the reported data. Secondly, the temperatures were measured at the wall which are likely to be influenced more by the heat inleak than the actual process dynamics considered for modeling. However, the matching of the trend indicates the success of the model for predicting the trend correctly.

7. Conclusion

A novel lumped parameter model for injection cooling including the effects of bubble dynamics has been reported. The bubble hydrodynamics has been accounted based on gas holdup in the liquid and Sauter mean diameter. The simulation results show good agreement with the experimental results obtained from the literature. Thus the model is useful for quick analysis of the effects of various operating variables on the process performance.

Acknowledgments
Authors would like to acknowledge the financial supports by Liquid Propulsion Systems Centre, Indian Space Research Organization (ISRO), India, for carrying out this work.

Nomenclature

C_p	Isobaric specific heat
D_{AB}	Diffusion coefficient, A= liquid component, B = gas component
H_0	$H_0 = \frac{4}{3}\mathrm{EoMo}^{-0.149}\left(\frac{\mu_l}{\mu_w}\right)^{-0.14}$
H_l	Liquid height
K	Thermal conductivity
L	Length
T	Temperature
V_g	Total volume of gas phase
V_l	Total volume of liquid phase
V_t	Total volume of gas and liquid = $V_g + V_l$
$\dot{m}$	Mass transfer rate
$\dot{q}$	Heat transfer rate
a_s	Specific gas-liquid interfacial area
d	Diameter
d_{vs}	Volume-surface mean bubble diameter
g	Gravitational acceleration
h	Heat transfer coefficient
h_{fg}	Latent heat of vaporization
k	Mass transfer coefficient
m	Mass
$p_{A,b}$	Partial pressure of component A (liquid) inside bubble
$r_{ins,i}$	Inner radius of insulation
$r_{ins,o}$	Outer radius of insulation
t	Time
v_g	Superficial velocity of gas
v_t	Terminal rise velocity of bubble
${P_A}^{Sat}$	Saturation pressure of component A (liquid)

Dimensionless Numbers

Bo	Bond Number = $\frac{{d_c}^2 \rho_l}{\sigma}$
Eo	Eotvos number = $\frac{g(\rho_l - \rho_g){d_{vs}}^2}{\sigma}$
Fr	Froude number = $\frac{v_g}{\sqrt{g d_c}}$
Ga	Galilei number = $\frac{g {d_c}^3 {\rho_l}^2}{{\mu_l}^2}$
Mo	Morton number = $\frac{g {\mu_l}^4 (\rho_l - \rho_g)}{{\rho_l}^2 \sigma^3}$
Pr	Prandtl number = $\frac{C_{p,l}\mu_l}{K_l}$
Re_c	Reynolds number for continuous phase = $\frac{\rho_l v_g d_b}{\mu_l}$
Re_d	Reynolds number for dispersed phase = $\frac{\rho_g v_b d_b}{\mu_g}$
Sc	Schmidt number = $\frac{\mu_g}{\rho_g D_{\mathrm{AB}}}$
Sh	Sherwood number = $\frac{k_g d_b}{D_{\mathrm{AB}}}$
St	Stanton number = $\frac{h_l}{\rho_l C_{p,l} v_g}$

Greek Symbols

ϵ_g	Gas holdup
μ	Viscosity
ρ	Density
σ	Surface tension
τ	Tortuosity factor

Subscripts

amb	Ambient
c	Column
evp	Evaporation
g	Gas
ins	Insulation
l	Liquid
w	Water

References

[1] Ewart R O and Dergance R H 1978 Cryogenic propellant densification study Tech. Rep. NASA-CR-159438, MCR-78-586 Martin Marietta Corp. Denver, CO, United States

[2] Moran M, Haberbusch M, Satornino G, Moran M, Haberbusch M and Satornino G 1997 Joint Propulsion Conferences (American Institute of Aeronautics and Astronautics)

[3] Xie F, Li Y, Wang L and Ma Y 2017 *Applied Thermal Engineering* **118** 82 – 89

[4] Mustafi S, Canavan E, Johnson W, Kutter B and Shull J 2009 AIAA SPACE Forum (American Institute of Aeronautics and Astronautics)

[5] Mustafi S, Johnson W, Kashani A, Jurns J, Kutter B, Kirk D and Shull J 2010 AIAA SPACE Forum (American Institute of Aeronautics and Astronautics)

[6] Minkoff G J, Scherber F I and Stober A K 1957 *Nature* **180** 1413–1414

[7] Larsen P S, Randolph W O, Vaniman J L and Clark J A 1962 *Advances in Cryogenic Engineering* vol 8 ed Timmerhaus K D (Plenum Press) pp 507–520

[8] Schmidt A F 1962 *Advances in Cryogenic Engineering* vol 8 ed Timmerhaus K D (Plenum Press) pp 521–528

[9] Yudaev B N, Tsirlin O V and Yushkin A A 1973 *Journal of Engineering Physics* **25** 1360–1365 ISSN 0022-0841

[10] Cho N, Kwon O, Kim Y and Jeong S 2006 *Cryogenics* **46** 132 – 142

[11] Jung Y, Cho N, Baek S and Jeong S 2014 *Cryogenics* **64** 272 – 282

[12] Ramesh T and Thyagarajan K 2014 *International Journal of Engineering and Technology* **6** 58–65

[13] Sandilya P, Saha P and Sengupta S 2015 *Physics Procedia* **67** 386 – 391 proceedings of the 25th International Cryogenic Engineering Conference and International Cryogenic Materials Conference 2014

[14] Viswanathan K and Rao D S 1984 *Chemical Engineering Communications* **25** 133–155

[15] Akita K and Yoshida F 1974 *Industrial & Engineering Chemistry Process Design and Development* **13** 84–91

[16] Clift R, Grace J R and Weber M E 2005 *Bubbles, Drops, and Particles* Dover Civil and Mechanical Engineering Series (Dover Publications) ISBN 9780486445809

[17] Deckwer W D 1980 *Chemical Engineering Science* **35** 1341 – 1346

[18] Saboni A, Alexandrova S, Karsheva M and Gourdon C 2016 *Chemical Engineering Science* **152** 109 – 115